ORIGINAL RESEARCH

Tumor Growth Pattern and Intra- and Peritumoral Radiomics Combined for Prediction of Initial TACE Outcome in Patients with Primary Hepatocellular Carcinoma

Jiaying Li[1,2,*], Minhui Zhou[2,*], Yahan Tong[3], Haibo Chen[1], Ruisi Su[2], Yinghui Tao[2], Guodong Zhang[1], Zhichao Sun[1]

[1]Department of Radiology, The First Affiliated Hospital of Zhejiang Chinese Medical University (Zhejiang Provincial Hospital of Chinese Medicine), Hangzhou, 310006, People's Republic of China; [2]The First Clinical Medical College of Zhejiang Chinese Medical University, Hangzhou, 310053, People's Republic of China; [3]Department of Radiology, The Cancer Hospital of the University of Chinese Academy of Sciences (Zhejiang Cancer Hospital), Hangzhou, 310005, People's Republic of China

*These authors contributed equally to this work

Correspondence: Zhichao Sun, Department of Radiology, The First Affiliated Hospital of Zhejiang Chinese Medical University (Zhejiang Provincial Hospital of Chinese Medicine), 54 Youdian Road, Hangzhou, People's Republic of China, Tel/Fax +86-571-87077272, Email sunzhichao@zcmu.edu.cn

Purpose: Non-invasive methods are urgently needed to assess the efficacy of transarterial chemoembolization (TACE) and to identify patients with hepatocellular carcinoma (HCC) who may benefit from this procedure. This study, therefore, aimed to investigate the predictive ability of tumor growth patterns and radiomics features from contrast-enhanced magnetic resonance imaging (CE-MRI) in predicting tumor response to TACE among patients with HCC.

Patients and Methods: A retrospective study was conducted on 133 patients with HCC who underwent TACE at three centers between January 2015 and April 2023. Enrolled patients were divided into training, testing, and validation cohorts. Rim arterial phase hyperenhancement (Rim APHE), tumor growth patterns, nonperipheral washout, markedly low apparent diffusion coefficient (ADC) value, intratumoral arteries, and clinical baseline features were documented for all patients. Radiomics features were extracted from the intratumoral and peritumoral regions across the three phases of CE-MRI. Seven prediction models were developed, and their performances were evaluated using receiver operating characteristic (ROC) and decision curve analysis (DCA).

Results: Tumor growth patterns and albumin-bilirubin (ALBI) score were significantly correlated with tumor response. Tumor growth patterns also showed a positive correlation with tumor burden (r = 0.634, P = 0.000). The Peritumor (AUC = 0.85, 0.71, and 0.77), Clinics_Peritumor (AUC = 0.86, 0.77, and 0.81), and Tumor_Peritumor (AUC = 0.87, 0.77, and 0.80) models significantly outperformed the Clinics and Tumor models (P < 0.05), while the Clinics_Tumor_Peritumor model (AUC = 0.88, 0.81, and 0.81) outperformed the Clinics (AUC = 0.67, 0.77, and 0.75), Tumor (AUC = 0.78, 0.72, and 0.68), and Clinics_Tumor (AUC = 0.82, 0.83, and 0.78) models (P < 0.05 or 0.053, respectively). The DCA curve demonstrated better predictive performance within a specific threshold probability range for Clinics_Tumor_Peritumor.

Conclusion: Combining tumor growth patterns, intra- and peri-tumoral radiomics features, and ALBI score could be a robust tool for non-invasive and personalized prediction of treatment response to TACE in patients with HCC.

Keywords: hepatocellular carcinoma, radiomics, tumor growth pattern, transarterial chemoembolization

Introduction

Hepatocellular carcinoma (HCC) is the sixth most common malignant tumor globally and the third leading cause of cancer-related deaths.[1] Approximately 80% of patients with HCC are diagnosed with intermediate to advanced unresectable lesions.[2,3] According to the Barcelona Clinic Cancer (BCLC) staging system, transcatheter arterial

chemoembolization (TACE) is a crucial treatment for patients with intermediate-stage HCC.[4,5] In clinical practice, TACE is commonly applied in a multitude of clinical scenarios, particularly in Asian countries.[6,7] However, the efficacy of TACE is typically evaluated based on radiological tumor response one month after treatment.[8,9] Several studies have shown that the initial response to TACE is an independent prognostic factor for clinical outcomes and influences personalized treatment strategies for patients with HCC.[10,11] As such, early identification of key factors that may predict response to TACE is crucial for the comprehensive management of patients with HCC.

Tumor burden is an important factor in selecting suitable patients for TACE.[12] Some patients may not benefit from TACE due to factors such as excessive tumor burdens and poor liver function statuses (eg, Child-Pugh stage, ALBI score, etc).[9] High tumor burden considerably influences the subclassifications or prediction models used to stratify patients unsuitable for TACE.[13] Based on the 7–11 tumor burden criteria by Hung et al,[14,15] incomplete HCC capsule and radiological patterns suggesting potential vascular invasion are crucial factors influencing TACE response. An incomplete tumor capsule is characterized by multinodular, massive, infiltrative, and extranodular growth patterns, indicating a higher risk of vascular invasion which can result in reduced efficacy of TACE.[16] This is due to a partial blood supply from the portal veins rather than the hepatic arteries in these tumors. Different tumor growth patterns can also considerably impact treatment outcomes following the initial and subsequent TACE procedures.[15,16]

Radiomics, defined as the extraction of high-throughput features from medical images, is an emerging tool applied to code tumor phenotype, quantitatively assess tumor biological heterogeneity, and evaluate preoperative survival rates. This technique has demonstrated considerable potential to advance precision medicine.[17] Radiomics shows better predictive abilities for treatment response and tumor recurrence following TACE in HCC patients compared to traditional imaging methods. Various studies have confirmed the feasibility of using radiomics in these approaches.[18–20] The efficacy of TACE treatment depends on the internal heterogeneity of tumors and their peripheral area. Biological invasion, microinvasion, and micrometastasis can further change the tumor microenvironment, impacting treatment results. Changes in the peripheral area, such as peripheral arterial enhancement, irregularity at the tumor edges, and peritumoral microsatellite distribution, are all effective predictors of HCC recurrence.[21–23] Recent studies have shown that peritumoral radiomics models are more effective than intratumoral radiomics in assessing recurrence-free survival and early recurrence following HCC resection and ablation.[23,24] Peritumoral radiomics features and tumor growth patterns may also be closely linked to the clinical prognosis of TACE, as indicated by the findings above. In general clinical practice, magnetic resonance imaging (MRI) plays a crucial role in tumor staging, treatment strategy planning, and assessment of treatment response.

Given the above context, the present study aimed to create a new model predicting the efficacy of TACE as the primary treatment for HCC through the analysis of tumor growth patterns and MRI radiomics within and around the tumor. This model thus aims to offer personalized pre-treatment assessment of TACE response in liver cancer patients and to assess its potential for clinical use.

Materials and Methods
Patient Characteristics
This study was approved by the institutional review board of the First Affiliated Hospital of Zhejiang Chinese Medical University (No. 2022-KLS-185-01). The need for written informed consent was waived due to the retrospective study design. All the clinical data were collected and reviewed confidentially from the hospital's electronic database. All procedures involving human participants were conducted in accordance with the Declaration of Helsinki.

This study enrolled patients with HCC who presented to our institute from January 2015 to April 2023 and met the following specific inclusion criteria: (a) age ≥18 years; (b) received TACE treatment; (c) liver function categorized as Child-Pugh A or B; (d) Eastern Cooperative Oncology Group (ECOG) performance status score ranging from 0 to 2; (e) expected survival duration > 3 months; and (f) underwent contrast-enhanced MRI (CE-MRI) within a month prior to TACE. The diagnosis of HCC was confirmed either histopathologically, or by using the non-invasive criteria defined by the American Association for the Study of Liver Disease, which relies on specific imaging features.[3]

The exclusion criteria included: (a) history of prior treatment for HCC (eg, TACE, ablation, chemotherapy, etc).; (b) previous or current malignancy other than HCC; (c) intraoperative simultaneous ablation procedure; (d) receipt of any adjuvant therapy (eg, immunotherapy, chemotherapy, etc.) within 3 months post-TACE; (e) poor quality MR images for analysis (eg, severe artifacts or incomplete sequences); and (f) absence of short-term follow-up information. The patient selection process is illustrated in Figure 1.

MR Data Acquisition

MRI examinations were performed using 1.5 T (Syngo MR B17, Siemens) or 3.0 T MR systems (Discovery MR 750, GE Healthcare; Verio MR, Siemens), with a body array coil. The imaging protocol comprised T1-weighted (T1W), T2-weighted (T2W), diffusion-weighted imaging (DWI), and CE-MRI, with fat-suppressed T1-weighted three-dimensional (3D) fast-spoiled gradient-recalled echo sequence. The arterial phase (AP), portal venous phase (PVP), and delayed venous phase (DP) images were acquired during suspended respiration at 25–35s, 50–60s, and 150–240s following the administration of gadolinium-diethylenetriamine pentaacetic acid (Gd-DTPA) (Bayer Schering Pharma AG), respectively. Gd-DTPA was administered via the median cubital vein at a weight-dependent dose of 0.2 mL/kg and an injection rate of 2 mL/s. The detailed parameters for each scan sequence are listed in Supplementary Data S1.

Baseline Evaluation

Data on the demographic profiles, tumor characteristics, and various biochemistry data points, including age, gender, hepatitis B or C infection, serum alpha-fetoprotein (AFP), total bilirubin (TBIL), albumin (ALB), prothrombin time (PT), alanine aminotransferase (ALT), aspartate aminotransferase (AST), platelet count (PLT), neutrophil count, lymphocyte count, monocyte count, C-reactive protein (CRP), Child-Pugh class, ALBI score, and BCLC stage were collected. Patient performance status was assessed using the ECOG performance scale. The albumin-bilirubin (ALBI) score was further calculated using the formula: linear predictor (xb) = (log10 bilirubin μmol/L × 0.66) + (albumin g/L × −0.085).[25] Additionally, the inflammatory burden index (IBI) and neutrophil-lymphocyte ratio (NLR) were calculated.[26] The IBI was calculated using the following formula: CRP × neutrophil /lymphocyte. Finally, the NLR was calculated by dividing the neutrophil count by the lymphocyte count.
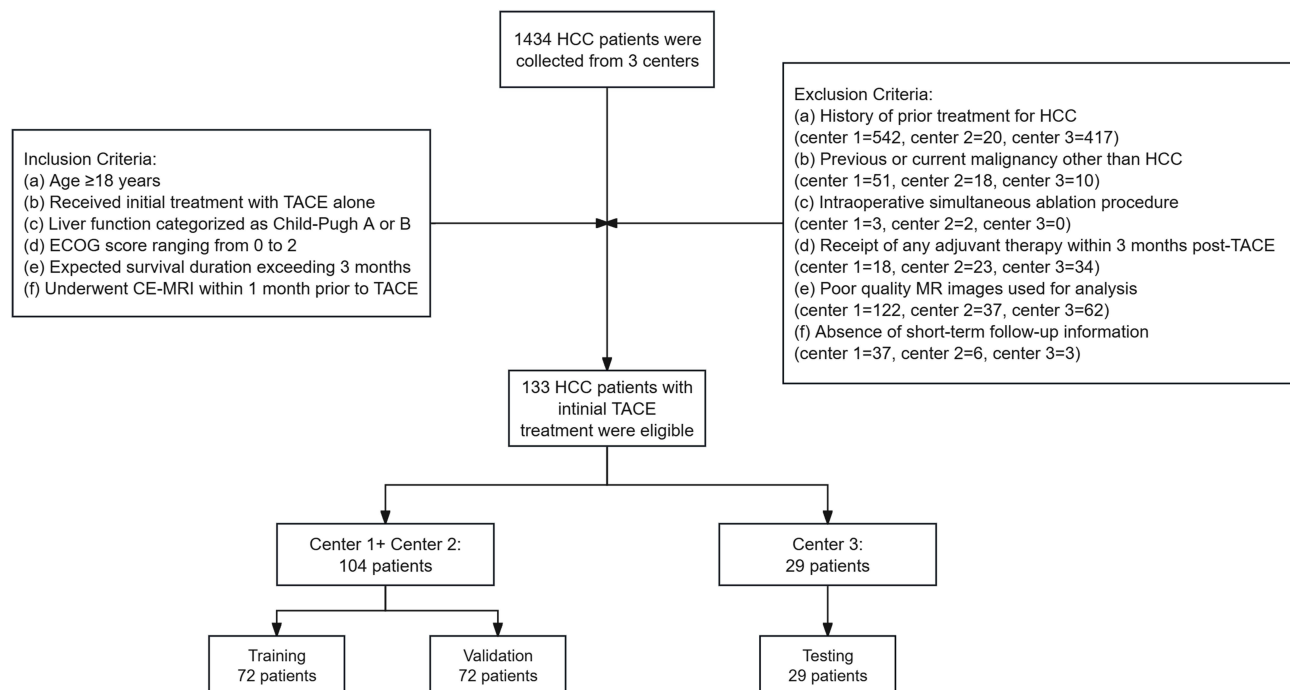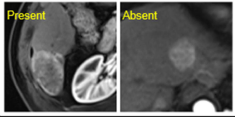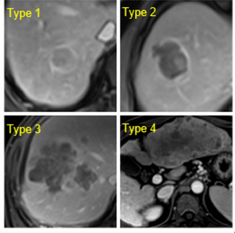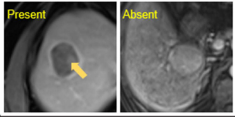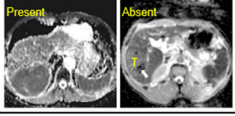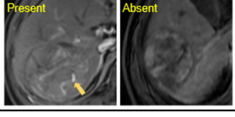

Figure 1 A flowchart of participant enrollment.

Radiological Image Analysis

The radiological analysis included evaluation of the tumor number, tumor size, tumor burden and radiological features. The tumor burden was calculated by summing the total number of tumors and the maximum tumor diameter, and was classified as a low, medium or high burden based on the 7–11 criteria (<7, 7–11, and >11, respectively).[14] The documented tumor-related prognostic radiological features include the Rim arterial phase hyperenhancement (Rim APHE), tumor growth patterns, nonperipheral washout, markedly low ADC value, and intratumoral arteries (Figure 2).[27] The Rim APHE feature is a subtype of the arterial phase hyperenhancement characterized by the most pronounced enhancement in the tumor's periphery. The tumor growth patterns can be categorized into four types: type 1, single nodular type - a round expanding nodule with a distinct margin observed in all imaging planes; type 2, single nodule type with extranodular growth - an expanding nodule with regions of bulging or nodular extranodular projection, involving less than 50% of the tumor circumference; type 3, confluent multinodular type - a cluster of small and confluent nodules; and type 4, infiltrative type - a tumor with extranodular growth involving more than 50% of circumference. The nonperipheral washout was visually assessed as a nonperipheral temporal reduction in tumor enhancement compared to the surrounding liver tissue in portal venous phase or delayed phase. A markedly low apparent diffusion coefficient (ADC) value was defined as a value comparable to or lower than that of the non-iron-overloaded spleen. The presence of discrete arteries within the tumor on arterial phase images indicates the existence of intratumoral arteries. All MRI images were independently reviewed by an abdominal radiologist with 8 years of experience, with classifications verified by another abdominal radiologist with 15 years of experience. In case of disagreement, a third radiologist with 28 years of experience was invited to confirm the final diagnosis.

Treatment Procedure and Outcome Evaluation

The TACE procedures were conducted by experienced senior physicians with over 10 years of expertise in interventional therapy. The TACE procedure is detailed in Supplementary Data S2. The response to TACE treatment was assessed using

Radiologic features	Definitions	Illustrations
Rim APHE	Spatially defined subtype of arterial phase hyperenhancement in which arterial phase enhancement is most pronounced in tumor periphery.	
Tumor growth subtypes	Type 1, single nodular type:a round expanding nodule with a distinct margin in all imaging planes; Type 2, single nodule type with extranodular growth: an expanding nodule with regions of bulging or nodular extranodular projection involving less than 50% of the tumor circumference; Type 3, confluent multinodular type: a cluster of small and confluent nodules; Type 4, infiltrative type: tumor with extranodular growth involving more than 50% of circumferce.	
Nonperipheral washout	Nonperipheral visually assessed temporal reduction in enhancement of the tumor in whole or in part relative to composite liver tissue in portal venous phase or delayed phase (yellow arrow means nonperipheral washout).	
Markedly low ADC value	Apparent diffusion coefficient value of the tumor comparable or lower than that of the non-iron-overloaded spleen. (T, tumor; white arrow means bleeding foci)	
Intratumoral arteries	Presence of discrete arteries (yellow arrow) within the tumor on arterial phase images.	

Figure 2 The definitions and illustrations of the tumor-related prognostic radiological features.
Abbreviations: APHE, arterial phase hyperenhancement; ADC, apparent diffusion coefficient.

the modified Response Evaluation Criteria in Solid Tumors (mRECIST) criteria,[28] which classifies responses as: complete response (CR), partial response (PR), stable disease (SD), or progression disease (PD). The objective response rate (ORR) was calculated by adding the CR and PR, while the non-response rate (NRR) was determined by adding SD and PD. Radiological tumor response was evaluated through contrast-enhanced CT or MRI scans performed 1 to 3 months following the initial TACE procedure. If viable or residual tumors were observed, on-demand TACE or alternative modalities such as surgery, radiation therapy, systemic therapy, etc., were considered for optimal therapy when other treatment options were deemed unsuitable for the patient.

Tumor Segmentation and Extraction of Radiomics Features

The preoperative CE-MRI images (AP, PVP, DP) were exported in DICOM format and loaded into the open-source software 3D Slicer (version 5.4.0, http://www.slicer.org/) for three-dimensional segmentation. The entire volume of interest (VOI_intratumor) was manually delineated around the complete tumor outline on each axial slice. The volume of interest (VOI) 5 mm from the tumor surface was defined as the peritumoral zone (VOI_peritumor). In cases of multiple lesions, only the largest lesions were selected. The delineation of all VOIs was performed independently by two abdominal radiologists with 7 and 10 years of experience. The inter-observer repeatability was evaluated using the intra-class correlation coefficient (ICC). All radiomics features were extracted from the intratumoral and peritumoral VOIs using the pyradiomics package (http://www.radiomics.io/pyradiomics.html). A total of 3999 radiomic features were extracted for each VOI from the AP, PVP, and DP images. The extracted radiomic features encompassed tumor intensity, texture, and shape from the unfiltered and filtered images using various filtering techniques and wavelet-based methods. The VOI segmentation diagram is presented in Figure 3.

Feature Selection and Model Construction

The extracted radiomics features underwent additional processing for further analysis. The data was standardized, and abnormal values were replaced with the median values of all parameters. To achieve dimension reduction, an XG-Boost
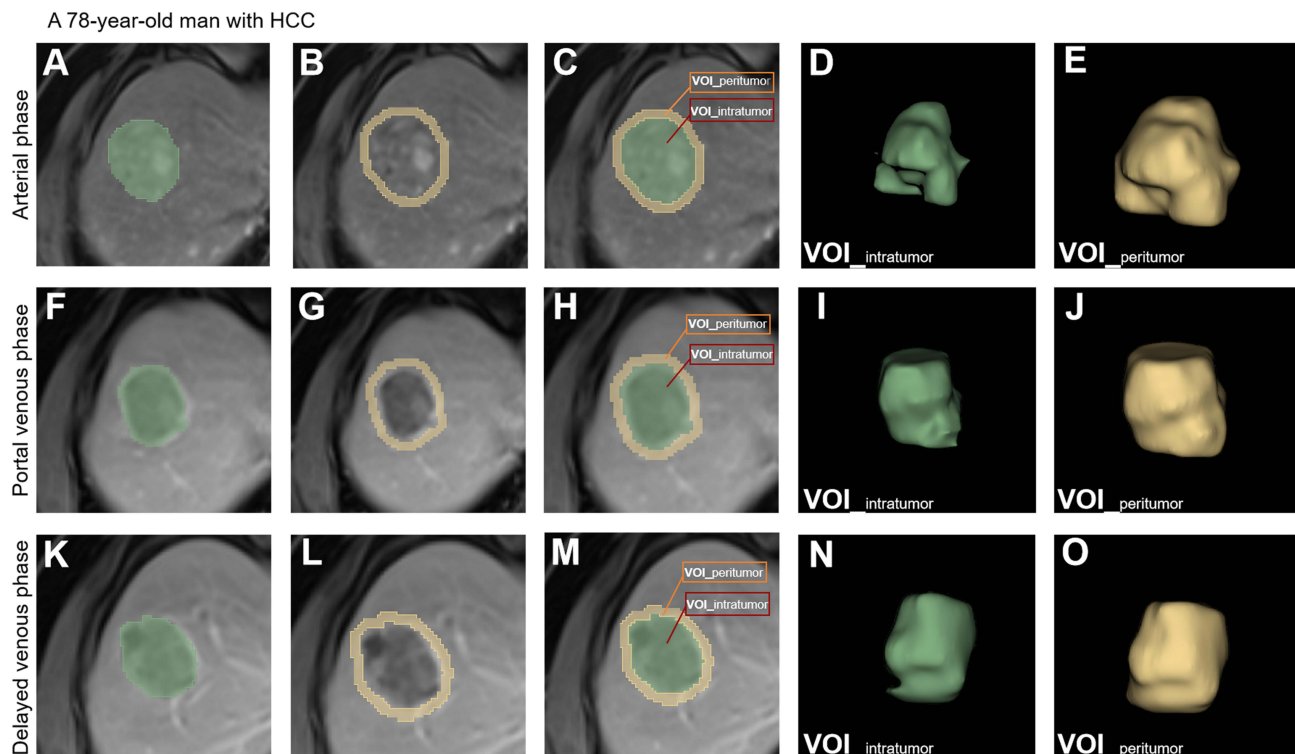
Figure 3 Exemplar diagram of VOI segmentation, showing the segmentation of volumes of interest (VOI) in various phases of MRI images: arterial phase (**A–C**), portal venous phase (**F–H**), and delayed venous phase (**K-M**). The intratumoral VOI (**A, F, K** and **D, I, N**) is extended outward by 5mm to form the peritumoral VOI (**B, G, L** and **E, J, O**).

method was applied to select crucial radiomics features. The selected features were visually explained using the Shapley Additive exPlanations (SHAP) technique, a post hoc interpretability method based on game theory. SHAP values represent a quantification of the importance of each feature and its impact on the model's predicted probability.[29] The radiomics models were constructed using random forest (RF) methods with chosen features from intratumoral and peritumoral regions in the training cohort, yielding a radscore for each model (Tumor and Peritumor models). The clinical-radiological (Clinics) model was developed using logistic regression, incorporating independent clinical and radiological indicators. To enhance model performance, combined models were created by logistic regression to incorporate clinical, radiological, and radscore data. The categories included Tumor_Peritumor, Clinics_Tumor, Clinics_Peritumor, and Clinics_Tumor_Peritumor. A predictive nomogram based on Clinics_Tumor_Peritumor was developed to calculate the risk score. The performance of all of the constructed models was validated in the validation and testing cohorts. The workflow for model construction is illustrated in Figure 4.
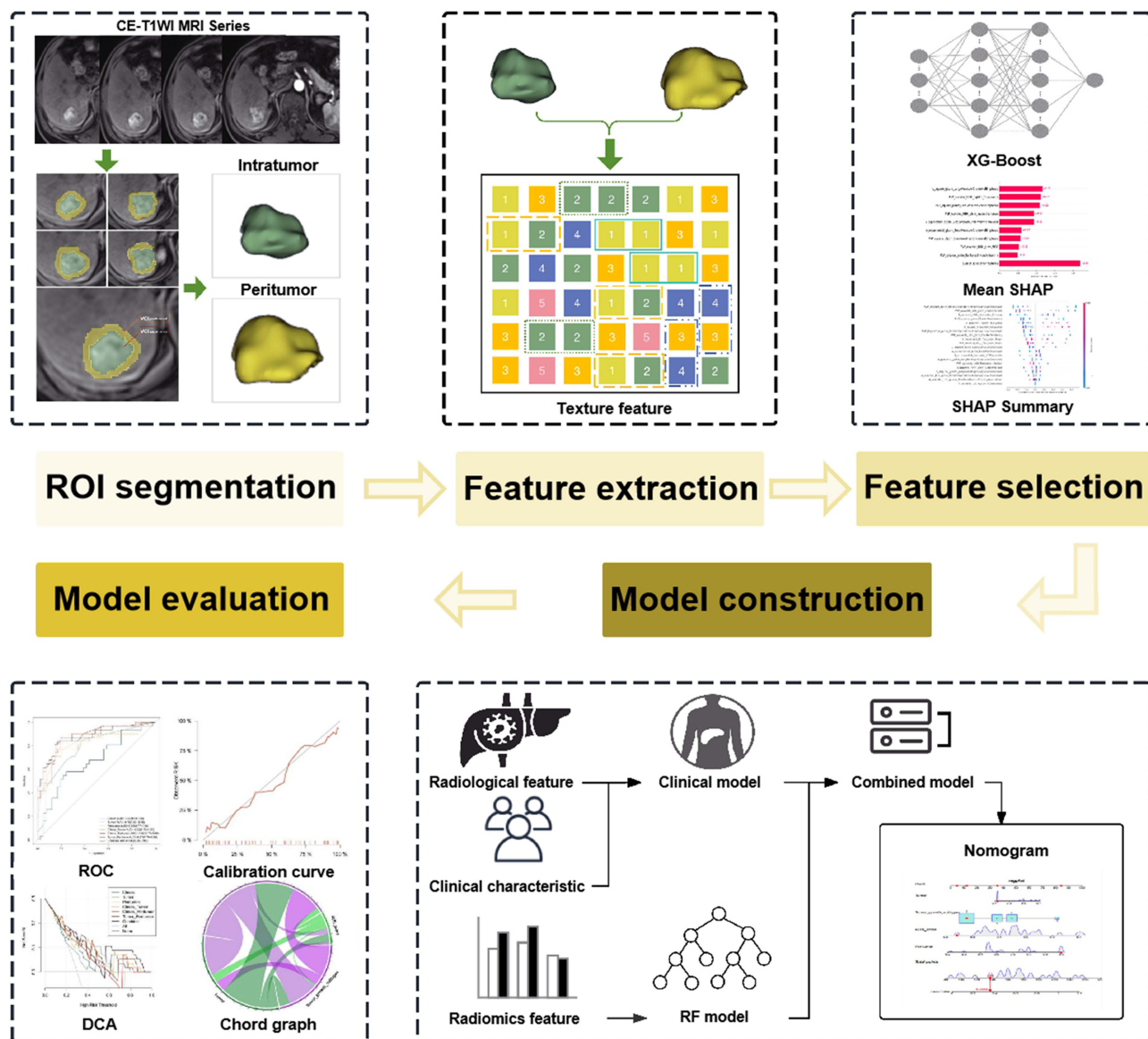

Figure 4 The workflow of the model construction process.

Statistical Analysis

The statistical analyses were conducted using R software (version 3.6.1, http://www.Rproject.org). Continuous variables were compared using the Student's *t*-test or Mann–Whitney *U*-test, while categorical variables were compared using the Chi-squared test or Fisher's exact test. Clinical indicators associated with tumor response were analyzed using the Akaike Information Criterion (AIC) model from the MASS package, followed by stepwise logistic regression modeling based on the precise AIC criteria. The correlation among specific clinical, radiological, intratumoral, and peritumoral radiomics scores was illustrated using a chord diagram, and the performances of the models were assessed using receiver operating characteristic (ROC) curve analysis. The area under the curve (AUC), accuracy, sensitivity, and specificity values were calculated for each ROC curve. DeLong's test was applied to compare AUCs of different models, while calibration curves were created to evaluate the model's predictive accuracy. Decision curve analysis (DCA) was finally conducted to assess the clinical utility at different threshold probabilities. Statistical significance was set at a two-sided P value < 0.05.

Results

Patient Characteristics

A total of 133 patients (median age, 61.5 years; range, 28–90 years), comprising 18% females (24/133) and 82% males (109/133), were enrolled. All patients were divided into training, validation, and testing groups. The training group consisted of 72 patients with a median age of 62.0 years, including 22.2% (16/72) females and 77.8% (56/72) males. The validation group included 32 patients with a median age of 64.1 years, including 15.6% (5/32) females and 84.4% (27/32) males. The testing group comprised 29 patients with a median age of 57.2 years, including 10.3% (3/29) females and 89.7% (26/29) males. The treatment response rates for the TACE procedure, according to the mRECIST criteria, were as follows: CR 18.1% (24/133), PR 35.3% (47/133), SD 40.6% (54/133), and PD 6.0% (8/133). The detailed baseline characteristics of patients in the training and validation cohorts are summarized in Table 1.

Among the different radiological features, Rim APHE, nonperipheral washout, markedly low ADC values, and intratumoral arteries were observed in 15.0%, 93.2%, 65.4%, and 42.1% of patients. Classification of tumor growth patterns revealed that types 1, 2, 3, and 4 accounted for 38.4%, 33.8%, 13.5%, and 14.3%, respectively. According to the

Table 1 Baseline Characteristics of Patients in Training and Validation Cohorts

Characteristics	Overall	Training Group	Validation Group	P. Value
n	104	72	32	
Age, mean (SD)	62.7 (12.1)	62.0 (11.9)	64.1 (12.7)	0.449
Sex, n (%)				0.611
Female	21 (20.2)	16 (22.2)	5 (15.6)	
Male	83 (79.8)	56 (77.8)	27 (84.4)	
MR_type, n (%)				0.500
1.5T	29 (27.9)	22 (30.6)	7 (21.9)	
3.0T	75 (72.1)	50 (69.4)	25 (78.1)	
Tumor_number, n (%)				0.521
1	57 (54.8)	38 (52.8)	19 (59.4)	
2	12 (11.5)	10 (13.9)	2 (6.2)	
≥3	35 (33.7)	24 (33.3)	11 (34.4)	
Tumor_size, mm, mean (SD)	68.2 (49.2)	68.1 (52.1)	68.5 (43.0)	0.961
Hepatitis, n (%)				0.125
Absent	30 (28.8)	17 (23.6)	13 (40.6)	
Present	74 (71.2)	55 (76.4)	19 (59.4)	
Cirrhosis, n (%)				0.545
Absent	49 (47.1)	32 (44.4)	17 (53.1)	

(*Continued*)

Table 1 (Continued).

Characteristics	Overall	Training Group	Validation Group	P. Value
Present	55 (52.9)	40 (55.6)	15 (46.9)	
AFP, ng/mL, mean (SD)	2820.1 (6084.9)	3038.5 (6222.2)	2328.7 (5830.0)	0.577
Albumin, g/L, mean (SD)	36.2 (6.3)	35.7 (6.7)	37.2 (5.3)	0.230
Total_bilirubin, μmol/L, mean (SD)	20.7 (12.4)	21.6 (13.7)	18.7 (8.7)	0.190
AST, U/L, mean (SD)	60.2 (82.6)	52.0 (48.0)	78.5 (130.1)	0.271
ALT, U/L, mean (SD)	41.4 (44.8)	36.1 (25.1)	53.2 (70.7)	0.193
NLR, mean (SD)	3.4 (2.9)	3.4 (2.6)	3.4 (3.4)	0.968
IBI, mean (SD)	92.3 (273.5)	88.9 (206.2)	99.9 (388.7)	0.880
Child_Pugh_score, n (%)				0.073
A	63 (60.6%)	43 (59.7%)	20 (62.5%)	
B	41 (39.4%)	29 (40.2%)	12 (37.5%)	
ALBI_score, mean (SD)	−2.3 (0.6)	−2.2 (0.6)	−2.4 (0.5)	0.196
BCLC_stage, n (%)				0.342
A	39 (37.5)	30 (41.7)	9 (28.1)	
B	20 (19.2)	11 (15.3)	9 (28.1)	
C	43 (41.3)	30 (41.7)	13 (40.6)	
D	2 (1.9)	1 (1.4)	1 (3.1)	
Rim_APHE, n (%)				0.771
Absent	88 (84.6)	60 (83.3)	28 (87.5)	
Present	16 (15.4)	12 (16.7)	4 (12.5)	
Tumor_growth_pattern, n (%)				0.655
Type 1	44 (42.3)	33 (45.8)	11 (34.4)	
Type 2	31 (29.8)	21 (29.2)	10 (31.2)	
Type 3	17 (16.3)	10 (13.9)	7 (21.9)	
Type 4	12 (11.5)	8 (11.1)	4 (12.5)	
Nonperipheral_washout, n (%)				0.664
Absent	6 (5.8)	5 (6.9)	1 (3.1)	
Present	98 (94.2)	67 (93.1)	31 (96.9)	
Markedly_low_ADC_value, n (%)				0.599
Absent	38 (36.5)	28 (38.9)	10 (31.2)	
Present	66 (63.5)	44 (61.1)	22 (68.8)	
Intratumoral_artery, n (%)				0.933
Absent	64 (61.5)	45 (62.5)	19 (59.4)	
Present	40 (38.5)	27 (37.5)	13 (40.6)	

Abbreviations: ADC, apparent diffusion coefficient; AFP, α-fetoprotein; ALBI, albumin-bilirubin; ALT, alanine aminotransferase; AST, aspartate aminotransferase; BCLC, Barcelona Clinic Liver Cancer; IBI, inflammatory burden index; MR, magnetic resonance; NLR, neutrophil-lymphocyte ratio; Rim_APHE, Rim arterial phase hyperenhancement; SD, standard deviation.

7–11 criteria, 47.3% of the patients demonstrated a low tumor burden, while 22.6% and 30.1% of the patients exhibited intermediate and high tumor burdens, respectively.

Clinical and Radiological Features Associated with TACE Treatment Response

Two clinical and radiological factors, the ALBI score and tumor growth patterns, demonstrated a statistically significant correlation with tumor response, as determined by the AIC criteria and stepwise logistic regression analysis (Table 2). Following the initial TACE, patients with type 1 (encapsulated nodular type) showed the highest ORR at 45.1%, followed by those type 2 (simple nodular type with extranodular growth) at 39.4%. Types 3 (confluent multinodular type) and 4 (infiltrative type) showed significantly lower response rates at 11.3% and 4.2%, respectively (P=0.002, Figure 5a). Moreover, a majority of patients with a high tumor burden showed a poor treatment response (NRR=65.0%) (r=0.257, P=0.003; Table 3 and Figure 5b). The ALBI score of patients who achieved an ORR was significantly lower compared to

Table 2 Clinical Factor Associated with Treatment Response After Initial TACE

Variable	AIC	Estimate	Standard Error	t Value	P value
Tumor_growth_pattern	−27.10	0.11	0.05	2.19	0.03
ALBI score	−29.62	0.42	0.20	2.13	0.04

Abbreviations: AIC, Akaike Information Criterion; ALBI, albumin-bilirubin; TACE, transarterial chemoembolization.

non-responding patients (−2.4±0.6 vs −2.2±0.5, P=0.018; Figure 5c). Furthermore, a positive correlation was identified between the tumor growth patterns and tumor burden (r=0.634, P=0.000) (Table 3 and Figure 5d).

Selection and Visual Interpretation of Intratumoral and Peritumoral Radiomics Features

The ICCs for VOI segmentation were 0.80–0.91, 0.67–0.85, and 0.63–0.77 in the AP, PVP, and DP images, respectively. A total of 3999 intratumoral and peritumoral features were obtained through the extraction of radiomics features from enhanced three-phase images. The XG-Boost method was subsequently utilized for dimensionality reduction. Finally, 16 intratumoral features and 19 peritumoral features were identified, as shown in Figure 6a, b and Supplementary Data S3. To visually explain the selected radiomics features, we applied SHAP to show how these variables affect the prediction model for TACE efficacy. The SHAP value offers valuable insights into each feature's contribution to the final prediction model (Figure 5e–h). The chord diagram shows the interconnections among ALBI score, tumor growth patterns, and radiomics features in intratumoral and peritumoral regions, all with varying degrees of correlation (Figure 6c–e).

Model Construction and Evaluation for the Prediction of the Response to Initial TACE Treatment

We developed a total of seven prediction models. The clinical-radiological model (Clinics) was created using logistic regression with two independent risk factors (ALBI score and tumor growth types). By applying the three-tree RF method, we identified 16 intratumoral and 19 peritumoral features that notably influenced the splitting process, with 5 features making the most substantial contribution (Figure 6a and b). Subsequently, we further developed radiomics prediction models (Tumor and Peritumor) based on the selected radscore. Four additional models were built using the logistic regression method: Tumor_Peritumor, Clinics_Tumor, Clinics_Peritumor, and Clinics_Tumor_Peritumor. The formula for logistic regression models is available in Supplementary Data S4.

Among the different individual models, the Peritumor model significantly outperformed the Clinics model (AUC=0.85 vs 0.67, P=0.006). However, no statistically significant differences were found between the Peritumor and Tumor models (AUC=0.85 vs 0.78, P=0.191), or between the Tumor and Clinics models (P=0.181). When the peritumoral radscore was included in the combined model (Clinics_Peritumor and Tumor_Peritumor), we identified a significant performance improvement compared to the single Clinics and Tumor models (AUC=0.67 vs 0.86 and 0.78 vs 0.87; P=0.001 and 0.013). Additionally, we observed a slight performance enhancement for the Clinics_Tumor combined model (AUC=0.82 vs 0.88, P=0.053). The addition of the tumoral radscore further significantly enhanced the performance of the Clinics model (AUC=0.67 vs 0.82, P=0.012). The combined Clinics_Tumor_Peritumor model outperformed the individual Clinics and Tumor models (AUC=0.67 vs 0.88 and 0.78 vs 0.88, P=0.001 and 0.016, respectively). Table 4 and Figure 7a–c present the discriminative performance of the various prediction models. DeLong tests were applied to compare the model performances, as detailed in Supplementary Data S5.

The DCA curve showed a better predictive performance within a specific threshold probability range for all models compared to the alternative (gray line) or no treatment options (black line) (Figure 7d–f). Combining the Clinics_Tumor_Peritumor models resulted in considerable clinical benefits. Additionally, calibration curves constructed using our combined model revealed good agreement between the predicted and measured values across the training, validation, and testing cohorts (Figure 7g–i). Therefore, a comprehensive nomogram based on the
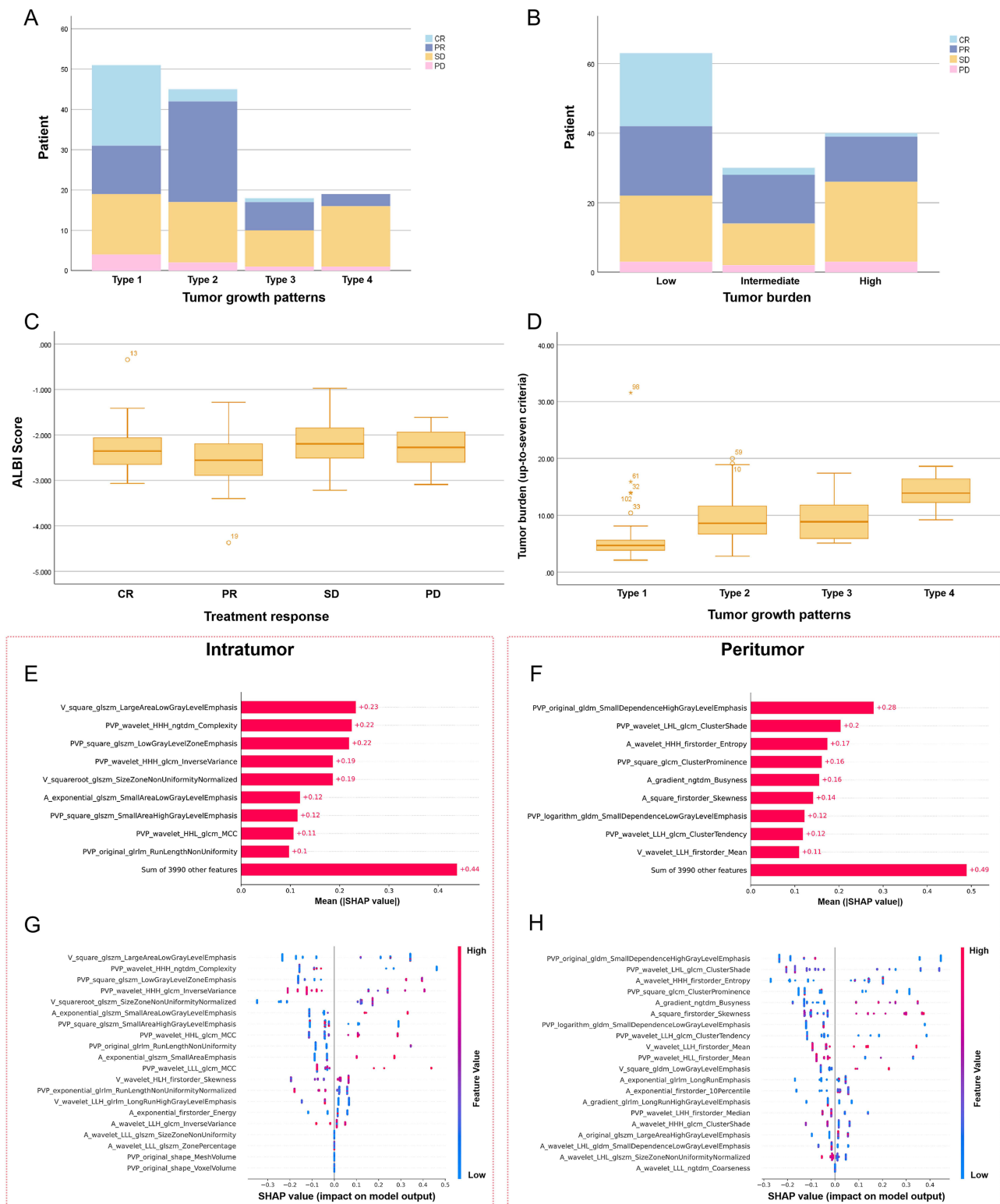
Figure 5 The stack bar chart, box plot, and SHAP visualization of clinical, radiological and radiomics features. (**A–D**) Stack bar chart (**A** and **B**) and box plot (**C** and **D**) showing the relationships between the ALBI score, tumor growth patterns, tumor burden, and TACE treatment response. (**E** and **F**) The mean |SHAP value| was used to rank the intratumoral and peritumoral radiomics features, identifying the top 10 features with the most considerable contributions to the model. (**G** and **H**) The top 20 most considerable and stable features were selected. Each point in the figure represents a sample, with redder colors indicating larger feature values and bluer colors indicating smaller feature values. The distribution of points indicates the magnitude of their influence on the final result. Even distribution of data points around the median line indicates a minimal impact of that particular feature. Notably, 16 intratumoral features and 19 peritumoral features showed the highest importance.

**Table 3** The Correlation Between Independent Risk Factors and Tumor Burden

Characteristics	Tumor Burden			r Value	P value
	Low	Intermediate	High		
Treatment response, n (%)	63 (47.3%)	30 (22.6%)	40 (30.1%)	0.257	0.003
ORR	41 (65.1%)	16 (53.3%)	14 (35.0%)		
NRR	22 (34.9%)	14 (46.7%)	26 (65.0%)		
ALBI_score, mean (SD)	−2.32 (0.62)	−2.46 (0.68)	−2.2 1(0.49)	0.073	0.403
Tumor_growth_pattern, n (%)				0.634	0.000
Type 1	44 (69.8%)	3 (10.0%)	4 (10.0%)		
Type 2	13 (20.6%)	20 (66.7%)	12 (30.0%)		
Type 3	6 (9.6%)	5 (16.7%)	7 (17.5%)		
Type 4	0 (0.0%)	2 (6.6%)	17 (42.5%)		

Abbreviations: ALBI, albumin-bilirubin; NRR, non-response rate; ORR, objective response rate.

Clinics_Tumor_Peritumor was developed to predict the risk of non-response in HCC patients following initial TACE treatment (Figure 8).

Discussion

Non-invasive imaging is important for predicting the survival of patients with HCC; however, there is currently no superior model for accurately predicting the efficacy of initial TACE treatment in this patient cohort. This study found that the clinical ALBI score and tumor growth pattern considerably influenced treatment response, with a strong correlation identified between tumor burden and treatment outcome. The performance of the Clinics model based on
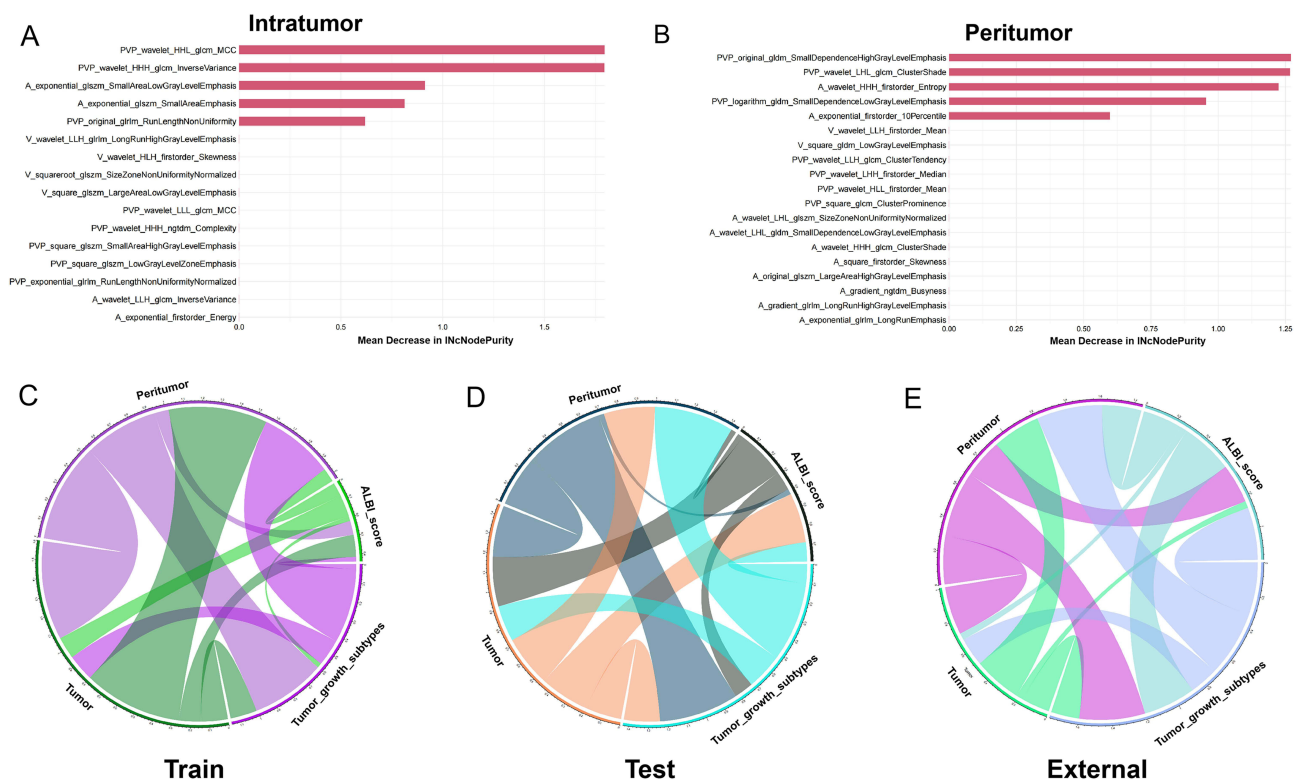
Figure 6 Weight bar chart of radiomics features and chord diagram for clinical, radiological and radiomics features. (**A** and **B**) The Mean Decrease in IncNodePurity was used as a metric to measure each variable's contribution in building each tree in the random forest. By using a three-tree random forest approach, 16 intratumoral and 19 peritumoral radiomics features that notably impact the process were identified. (**C–E**) The chord diagram shows the interrelation among ALBI score, tumor growth patterns, intratumoral and peritumoral radscore, all of which are correlated to varying degrees.

Table 4 Discrimination Performance of Different Predictive Models in the Training, Validation, and Testing Cohorts

| Model	Training Cohort					Validation Cohort					Testing Cohort				
	AUC	95% CI	ACC	TNR	TPR	AUC	95% CI	ACC	TNR	TPR	AUC	95% CI	ACC	TNR	TPR
Clinics	0.67	0.54–0.80	0.67	0.76	0.55	0.77	0.6–0.94	0.59	0.50	0.65	0.75	0.56–0.93	0.69	0.67	0.71
Tumor	0.78	0.67–0.89	0.69	0.68	0.71	0.72	0.54–0.91	0.59	0.67	0.53	0.68	0.50–0.86	0.63	0.50	0.78
Peritumor	0.85	0.77–0.94	0.79	0.83	0.74	0.71	0.53–0.89	0.72	0.58	0.82	0.77	0.59–0.95	0.66	0.72	0.57
Clinics_Tumor	0.82	0.72–0.93	0.74	0.71	0.77	0.83	0.68–0.98	0.76	0.83	0.71	0.78	0.61–0.96	0.66	0.86	0.86
Clinics_Peritumor	0.86	0.77–0.95	0.79	0.80	0.77	0.77	0.59–0.94	0.72	0.50	0.88	0.81	0.64–0.97	0.62	0.56	0.71
Tumor_Peritumor	0.87	0.79–0.96	0.79	0.76	0.84	0.77	0.59–0.95	0.72	0.82	0.82	0.80	0.63–0.96	0.69	0.71	0.71
Clinics_Tumor_Peritumor	0.88	0.79–0.96	0.82	0.78	0.87	0.81	0.65–0.97	0.76	0.75	0.76	0.81	0.65–0.97	0.75	0.72	0.78

Abbreviations: ACC, accuracy; AUC, area under curve; CI, confidence interval; TNR, specificity; TPR, sensitivity.
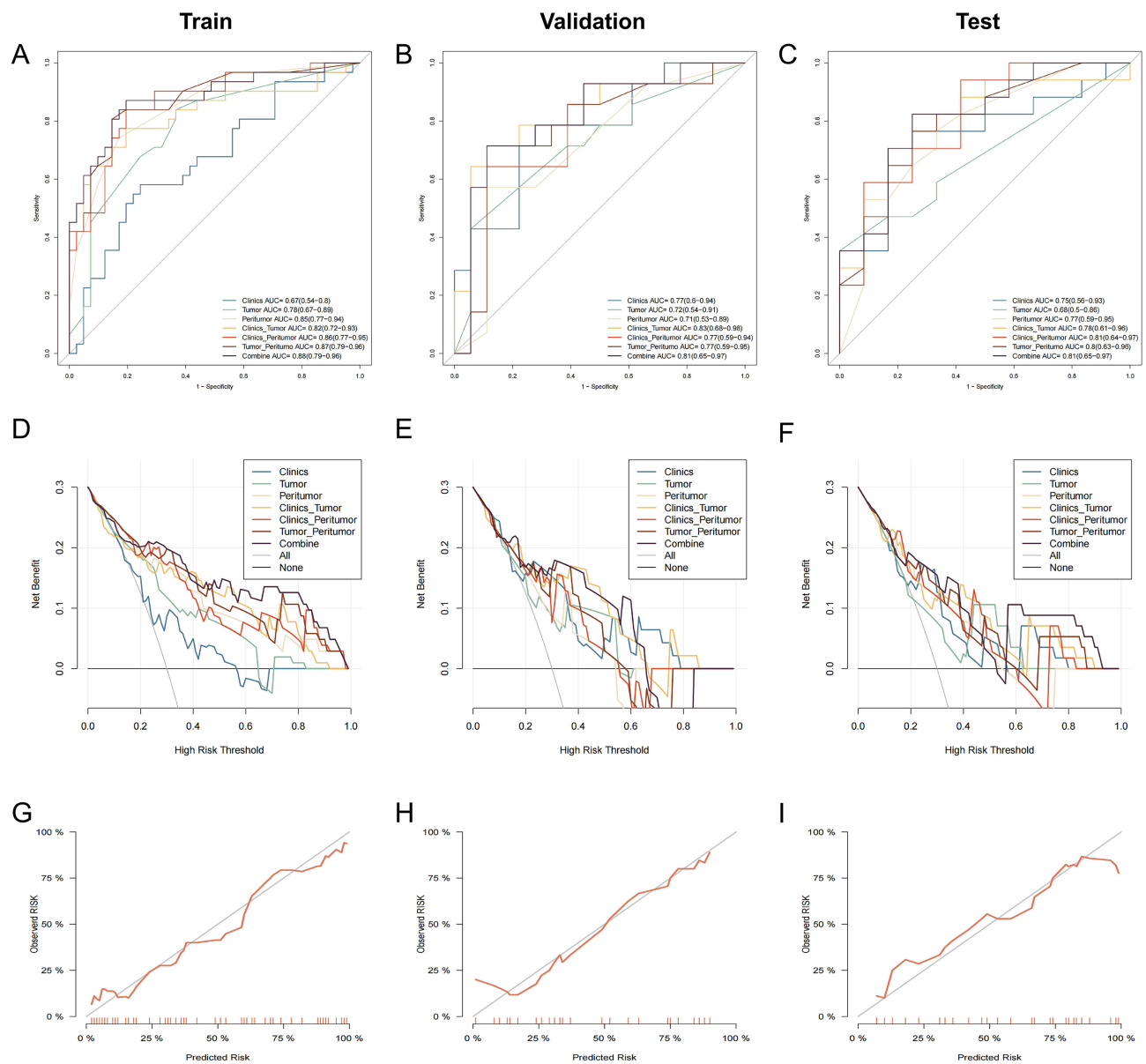
Figure 7 ROC, DCA and calibration curves for all models in the training cohort. In this study, participants were divided into training (**A, D, G**), validation (**B, E, H**), and testing (**C, F, I**) cohorts. (**D–F**) DCA curves showed that all models had strong predictive abilities for TACE response in HCC within a specific probability range compared to the different treatment regimens (gray line) or no treatment (black line). The Clinics_Tumor_Peritumor model further provided notable clinical benefits within a specific threshold. (**G-I**) The calibration curves of Clinics_Tumor_Peritumor showed excellent agreement between the predicted and measured values in the training, validation, and testing cohorts. In A-F "Combine" indicates the Clinics_Tumor_Peritumor model.

two clinical and radiological features was found to be suboptimal. However, the integration of intratumoral and peritumoral radiomics features from preoperative CE-MRI images enhanced predictive accuracy for non-response, particularly peritumoral features. Consequently, we developed integrated models to stratify patients based on specific clinical, radiological, and radiomics features. Overall, the combined nomogram model showed better risk stratification for TACE response than other models, aiding in the development of personalized clinical treatment decisions.

Several studies have suggested that a combined model is more valuable in assessing and predicting TACE outcomes in HCC patients. The integration of MRI radiomics features and clinical factors in the model showed a promising performance at predicting tumor treatment response, recurrence rate, and overall survival.[30–32] In one study assessing recurrence-free survival after TACE in HCC patients, Song et al[30] similarly found that the combined model outperformed the clinical-radiological and radiomics models. However, these integrated models did not account for radiological
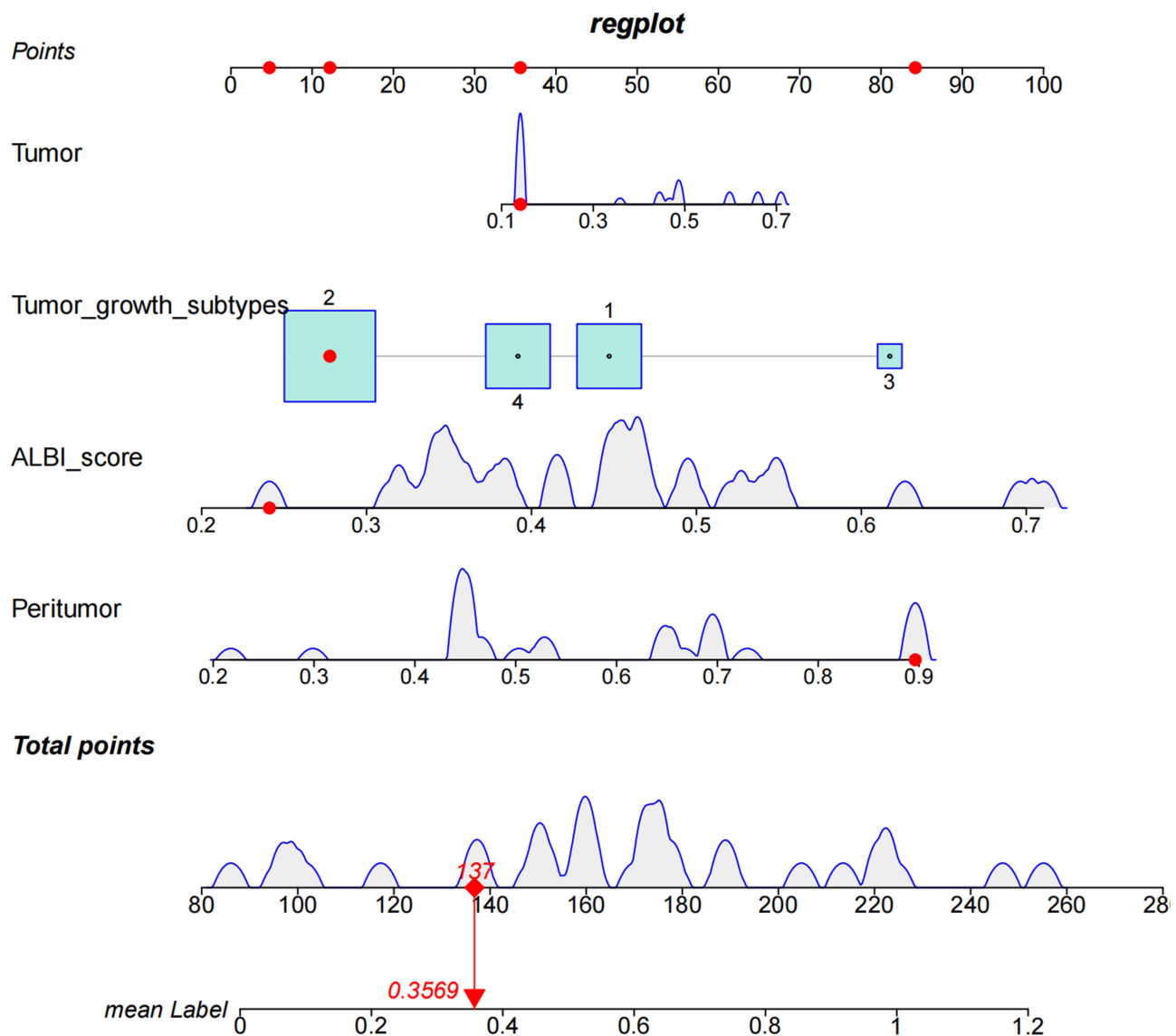
Figure 8 The combined nomogram incorporating the ALBI score, tumor growth patterns, intratumoral and peritumoral radscore characteristics to individually predict the risk of non-response in HCC patients following initial TACE treatment.

features linked to TACE prognosis. In our study, we examined the correlation between clinical, radiological, and radiomics features with treatment response. Logistic regression analyses identified ALBI scores and tumor growth patterns as independent predictors of ORR. The HAP score was found to be able to distinguish high- and low-risk HCC patients based on albumin and bilirubin levels.[12] The prognostic significance of the ALBI score, another quantitative indicator combining these levels, in HCC has previously been confirmed in several studies.[25,33,34] Radiological features are commonly applied to assess tumor prognosis due to their easy measurement and acquisition capabilities.[27] The tumor growth pattern is further crucial for predicting the prognosis of HCC patients undergoing TACE, as it is linked to the presence of a complete tumor capsule and the risk of vascular invasion. Specifically, various nodular fusion or infiltrating growth patterns, along with simple nodular growth accompanied by extraneous growth, can predict a poorer ORR and survival outcomes.[23] Our study confirmed earlier results showing that the confluent multi-nodular (type 3) and infiltrative (type 4) tumor types had lower ORRs of 11.3% and 4.2%, respectively, compared to simple nodular (type 1) and single nodule with extranodular growth (type 2) types, with response rates of 45.1% and

39.4% after initial TACE, respectively. Consequently, we hypothesized that the ALBI score and tumor growth pattern are crucial risk factors affecting the efficacy of TACE treatment, and are key predictors of ORR.

The 7–11 tumor criterion is a new method for predicting TACE response in HCC patients.[30] Our study confirmed the results of previous research showing that patients with a high tumor burden had a poor treatment response, with an NRR of 65.0%. We further found a statistically significant positive correlation between the tumor growth pattern and tumor burden. Consistent with previous studies,[15] we found that type 4 was correlated with high tumor burden, type 1 with low tumor burden, while type 2 (single nodule with extranodular growth) and 3 (confluent multinodular) fell in-between. Importantly, in cases where HCC presents with high tumor burden and unfavorable growth patterns, the efficacy and survival following TACE could be compromised, meaning that TACE should be avoided. The biological aggressiveness, micro-aggressiveness, and micrometastasis of tumors could also change the surrounding microenvironment.[30] Therefore, we extracted intratumoral and peritumoral radiomics features to more effectively capture tumor heterogeneity. Several studies have previously shown that using radiomics to assess tumor heterogeneity closely correlates with treatment response.[35,36] Pathologically, the tissue surrounding the tumor also shows tumor heterogeneity.[30,37,38] Our study showed that including the peritumoral radiomics features enhances the predictive accuracy of ORR after TACE, outperforming the clinical-radiological model and intratumoral radiomics model individually. These findings align with those of prior research.[23,24] By integrating intratumoral and peritumoral radiomics features, tumor heterogeneity could be effectively captured to predict outcomes in patients with HCC following TACE.

An et al[21] showed that Rim_APHE was an independent factor predicting early recurrence within 2 years following hepatectomy. Jiang et al[27] also found that Rim_APHE was linked to overall survival post-HCC surgery, while nonperipheral washout, markedly low ADC value, and intratumoral arteries were found to be linked to short-term recurrence-free survival. Conversely, our findings indicate that nonperipheral washout, markedly low ADC value, and intratumoral arteries are not reliable predictors of ORR. We speculated that this discrepancy may be due to the relatively small sample sizes and differences in treatment methods. Prior research has shown that serum inflammatory markers can indicate HCC recurrence.[39,40] The IBI is the most reliable biomarker for predicting tumor prognosis, showing superior results to existing systemic inflammation biomarkers. IBI allows the grading of inflammatory load in various malignant tumors using IBI scores. It further helps to predict post-hepatectomy survival in liver cancer patients, and enables effective prognostic stratification.[40] Our study showed that IBI cannot consistently predict outcomes, contradicting the results of prior research; as such, this point requires additional validation. These differences in serum markers may be due to selection bias, strict inclusion criteria, and possible interactions. Our clinical-radiological model showed an AUC of only 0.67, indicating limited preoperative assessment of tumor response following TACE using these factors.

The integrated model combining ALBI score, tumor growth pattern, and radiomics features within and around the tumor showed promising clinical utility and predictive accuracy. The nomogram further provides personalized treatment decisions to assess the objective response in patients with liver cancer after initial TACE treatment. Three phases of CE-MRI images were applied to identify and extract tumor treatment response, growth patterns, and intratumoral and peritumoral radiomics. MRI offers better tissue resolution than CT, particularly for tumor assessment. Some studies have applied non-enhanced T2WI, DWI, and other sequences to build prediction models;[41,42] however, their results often showed low AUC or specificity as concerns. CE-MRI primarily reflects tissue blood supply, with hepatic artery blood supply crucially affecting TACE efficacy.[41] Pre-treatment PVP imaging is more valuable for assessing tumor heterogeneity due to considerable signal differences caused by the washout characteristics during the PVP phase.[42] CE-MRI in the AP, PVP, and DP effectively capture essential radiological features, including lesion distribution, shape, margin, and blood supply dynamics,[42,43] thereby allowing the comprehensive assessment of lesion heterogeneity crucial for evaluating TACE treatment response. Previous studies have confirmed that the radiomics model is not affected by different magnetic field strengths when using various MRI scanners.[30] Mixed usage of MRI scanners is a common practice. All three phases (AP, PVP, DP) of CE-MRI sequences are essential for assessing TACE effectiveness and developing prediction models.

Our study has some limitations which should be mentioned. Firstly, the sample size was still relatively small, which may have limited the statistical robustness. Secondly, errors may have occurred in our assessment of viewer consistency,

as we performed manual mapping of lesion boundaries, which can be subjective. Thirdly, variations in TACE surgical procedures may exist among the different centers across which this study was conducted. Furthermore, this study is retrospective and may therefore have involved some selection bias. In future research, increasing the sample size and using a prospective methodology for model validation, along with integrating deep learning techniques for automatic region of interest delineation, will be crucial to enhance model robustness and generalizability.

Conclusion

In conclusion, this study introduces innovative strategies for the precise and individualized management of HCC patients. Based on our analyses, we propose a comprehensive model that integrates tumor growth patterns, intratumoral and peritumoral radiomics features from CE-MRI, along with the ALBI score to predict outcomes. Additionally, we developed a non-invasive nomogram based on the combined model to accurately predict tumor response in HCC patients following initial TACE treatment. Overall, these findings offer valuable insights into personalized clinical decision-making in this patient cohort.

Abbreviations

AASLD, American Association for the Study of Liver Disease; ADC, Apparent diffusion coefficient; AIC, Akaike Information Criterion; AP, Arterial phase; AUC, Area under the curve; BCLC, Barcelona Clinic Cancer; CR, Complete response; CRP, C-reactive protein; DCA, Decision curve analysis; DP, Delayed venous phase; DWI, Diffusion-weighted imaging; ECOG, Eastern Cooperative Oncology Group; IBI, Inflammatory burden index; ICC, Intra-class correlation coefficient; MRI, Magnetic resonance imaging; NLR, Neutrophil-lymphocyte ratio; NRR, Non-response rate; ORR, Objective response rate; PD, Progression disease; PR, Partial response; PT, Prothrombin time; PVP, Portal venous phase; RF, Random forest; ROC, Receiver operating characteristic; SD, Stable disease; TBIL, Total bilirubin; VOI, Volume of interest.

Data Sharing Statement

The datasets used and/or analyzed during the current study available from the corresponding author on reasonable request.

Ethics Approval and Informed Consent

This study was approved by the Institutional Review Board of The First Affiliated Hospital of Zhejiang Chinese Medical University. The need for informed consent was waived, and all methods were performed in accordance with the Declaration of Helsinki.

Acknowledgments

Author Contributions

All authors made a significant contribution to the work reported, whether that is in the conception, study design, execution, acquisition of data, analysis and interpretation, or in all these areas; took part in drafting, revising or critically reviewing the article; gave final approval of the version to be published; have agreed on the journal to which the article has been submitted; and agree to be accountable for all aspects of the work.

Funding

Disclosure

The authors report no conflicts of interest in this work.

References

1. Sung H, Ferlay J, Siegel RL, et al. Global Cancer Statistics 2020: GLOBOCAN Estimates of Incidence and Mortality Worldwide for 36 Cancers in 185 Countries. *CA Cancer J Clin.* 2021;71(3):209–249. doi:10.3322/caac.21660

2. European Association for the Study of the Liver. Electronic address: easloffice@easloffice.eu; European Association for the Study of the Liver. EASL Clinical Practice Guidelines: management of hepatocellular carcinoma [published correction appears in J Hepatol. 2019 Apr;70(4):817]. *J Hepatol.* 2018;69(1):182–236. doi:10.1016/j.jhep.2018.03.019.

3. Marrero JA, Kulik LM, Sirlin CB, et al. Diagnosis, Staging, and Management of Hepatocellular Carcinoma: 2018 Practice Guidance by the American Association for the Study of Liver Diseases. *Hepatology.* 2018;68(2):723–750. doi:10.1002/hep.29913

4. European Association For The Study Of The Liver; European Organisation For Research And Treatment Of Cancer. EASL-EORTC clinical practice guidelines: management of hepatocellular carcinoma [published correction appears in J Hepatol. 2012Jun; 56(6):1430]. *J Hepatol.* 2012;56 (4):908–943. doi:10.1016/j.jhep.2011.12.001.

5. Lencioni R, de Baere T, Soulen MC, Rilling WS, Geschwind JF. Lipiodol transarterial chemoembolization for hepatocellular carcinoma: a systematic review of efficacy and safety data. *Hepatology.* 2016;64(1):106–116. doi:10.1002/hep.28453

6. Chung GE, Lee JH, Kim HY, et al. Transarterial chemoembolization can be safely performed in patients with hepatocellular carcinoma invading the main portal vein and may improve the overall survival. *Radiology.* 2011;258(2):627–634. doi:10.1148/radiol.10101058

7. Yau T, Tang VYF, Yao T-J, Fan S-T, Lo C-M, Poon RTP. Development of Hong Kong Liver Cancer staging system with treatment stratification for patients with hepatocellular carcinoma. *Gastroenterology.* 2014;146(7):1691–700.e3. doi:10.1053/j.gastro.2014.02.032

8. Wang JH, Zhong XP, Zhang YF, et al. Cezanne predicts progression and adjuvant TACE response in hepatocellular carcinoma. *Cell Death Dis.* 2017;8(9):e3043. doi:10.1038/cddis.2017.428

9. Piscaglia F, Ogasawara S. Patient Selection for Transarterial Chemoembolization in Hepatocellular Carcinoma: importance of Benefit/Risk Assessment. *Liver Cancer.* 2018;7(1):104–119. doi:10.1159/000485471

10. Han G, Berhane S, Toyoda H, et al. Prediction of Survival Among Patients Receiving Transarterial Chemoembolization for Hepatocellular Carcinoma: a Response-Based Approach. *Hepatology.* 2020;72(1):198–212. doi:10.1002/hep.31022

11. Adhoute X, Penaranda G, Naude S, et al. Retreatment with TACE: the ABCR SCORE, an aid to the decision-making process. *J Hepatol.* 2015;62 (4):855–862. doi:10.1016/j.jhep.2014.11.014

12. Kadalayil L, Benini R, Pallan L, et al. A simple prognostic scoring system for patients receiving transarterial embolisation for hepatocellular cancer. *Ann Oncol.* 2013;24(10):2565–2570. doi:10.1093/annonc/mdt247

13. Koroki K, Ogasawara S, Ooka Y, et al. Analyses of Intermediate-Stage Hepatocellular Carcinoma Patients Receiving Transarterial Chemoembolization prior to Designing Clinical Trials. *Liver Cancer.* 2020;9(5):596–612. doi:10.1159/000508809

14. Hung YW, Lee IC, Chi CT, et al. Redefining Tumor Burden in Patients with Intermediate-Stage Hepatocellular Carcinoma: the Seven-Eleven Criteria. *Liver Cancer.* 2021;10(6):629–640. doi:10.1159/000517393

15. Hung YW, Lee IC, Chi CT, et al. Radiologic Patterns Determine the Outcomes of Initial and Subsequent Transarterial Chemoembolization in Intermediate-Stage Hepatocellular Carcinoma. *Liver Cancer.* 2023;13(1):29–40. doi:10.1159/000530950

16. Hashimoto T, Nakamura H, Hori S, et al. Hepatocellular carcinoma: efficacy of transcatheter oily chemoembolization in relation to macroscopic and microscopic patterns of tumor growth among 100 patients with partial hepatectomy. *Cardiovasc Intervent Radiol.* 1995;18(2):82–86. doi:10.1007/BF02807227

17. Lambin P, Leijenaar RTH, Deist TM, et al. Radiomics: the bridge between medical imaging and personalized medicine. *Nat Rev Clin Oncol.* 2017;14(12):749–762. doi:10.1038/nrclinonc.2017.141

18. Wang XH, Long LH, Cui Y, et al. MRI-based radiomics model for preoperative prediction of 5-year survival in patients with hepatocellular carcinoma. *Br J Cancer.* 2020;122(7):978–985. doi:10.1038/s41416-019-0706-0

19. Yao Z, Dong Y, Wu G, et al. Preoperative diagnosis and prediction of hepatocellular carcinoma: radiomics analysis based on multi-modal ultrasound images. *BMC Cancer.* 2018;18(1):1089. doi:10.1186/s12885-018-5003-4

20. Kim J, Choi SJ, Lee SH, Lee HY, Park H. Predicting Survival Using Pretreatment CT for Patients With Hepatocellular Carcinoma Treated With Transarterial Chemoembolization: comparison of Models Using Radiomics. *Am J Roentgenol.* 2018;211(5):1026–1034. doi:10.2214/AJR.18.19507

21. An C, Kim DW, Park YN, Chung YE, Rhee H, Kim MJ. Single Hepatocellular Carcinoma: preoperative MR Imaging to Predict Early Recurrence after Curative Resection. *Radiology.* 2015;276(2):433–443. doi:10.1148/radiol.15142394

22. Lee S, Kim SH, Lee JE, Sinn DH, Park CK. Preoperative gadoxetic acid-enhanced MRI for predicting microvascular invasion in patients with single hepatocellular carcinoma. *J Hepatol.* 2017;67(3):526–534. doi:10.1016/j.jhep.2017.04.024

23. Kim S, Shin J, Kim DY, Choi GH, Kim MJ, Choi JY. Radiomics on Gadoxetic Acid-Enhanced Magnetic Resonance Imaging for Prediction of Postoperative Early and Late Recurrence of Single Hepatocellular Carcinoma. *Clin Cancer Res.* 2019;25(13):3847–3855. doi:10.1158/1078-0432. CCR-18-2861

24. Shan QY, Hu HT, Feng ST, et al. CT-based peritumoral radiomics signatures to predict early recurrence in hepatocellular carcinoma after curative tumor resection or ablation. *Cancer Imaging.* 2019;19(1):11. doi:10.1186/s40644-019-0197-5

25. Johnson PJ, Berhane S, Kagebayashi C, et al. Assessment of liver function in patients with hepatocellular carcinoma: a new evidence-based approach-The ALBI grade. *J Clin Oncol.* 2015;33(6):550–558. doi:10.1200/JCO.2014.57.9151

26. Pinato DJ, Stebbing J, Ishizuka M, et al. A novel and validated prognostic index in hepatocellular carcinoma: the inflammation based index (IBI). *J Hepatol.* 2012;57(5):1013–1020. doi:10.1016/j.jhep.2012.06.022

27. Jiang H, Qin Y, Wei H, et al. Prognostic MRI features to predict postresection survivals for very early to intermediate stage hepatocellular carcinoma. *Eur Radiol.* 2023. doi:10.1007/s00330-023-10279-x

28. Llovet JM, Lencioni R. mRECIST for HCC: performance and novel refinements. *J Hepatol.* 2020;72(2):288–306. doi:10.1016/j.jhep.2019.09.026

29. Parsa AB, Movahedi A, Taghipour H, Derrible S, Mohammadian AK. Toward safer highways, application of XGBoost and SHAP for real-time accident detection and feature analysis. *Accid Anal Prev.* 2020;136:105405. doi:10.1016/j.aap.2019.105405

30. Song W, Yu X, Guo D, et al. MRI-Based Radiomics: associations With the Recurrence-Free Survival of Patients With Hepatocellular Carcinoma Treated With Conventional Transcatheter Arterial Chemoembolization. *J Magn Reson Imaging.* 2020;52(2):461–473. doi:10.1002/jmri.26977

31. Kong C, Zhao Z, Chen W, et al. Prediction of tumor response via a pretreatment MRI radiomics-based nomogram in HCC treated with TACE. *Eur Radiol*. 2021;31(10):7500–7511. doi:10.1007/s00330-021-07910-0

32. Liu QP, Yang KL, Xu X, Liu XS, Qu JR, Zhang YD. Radiomics analysis of pretreatment MRI in predicting tumor response and outcome in hepatocellular carcinoma with transarterial chemoembolization: a two-center collaborative study. *Abdom Radiol*. 2022;47(2):651–663. doi:10.1007/s00261-021-03375-3

33. Lee IC, Hung YW, Liu CA, et al. A new ALBI-based model to predict survival after transarterial chemoembolization for BCLC stage B hepatocellular carcinoma. *Liver Int*. 2019;39(9):1704–1712. doi:10.1111/liv.14194

34. Hsu CY, Lee YH, Hsia CY, et al. Performance status in patients with hepatocellular carcinoma: determinants, prognostic impact, and ability to improve the Barcelona Clinic Liver Cancer system. *Hepatology*. 2013;57(1):112–119. doi:10.1002/hep.25950

35. Ganeshan B, Miles KA. Quantifying tumour heterogeneity with CT. *Cancer Imaging*. 2013;13(1):140–149. doi:10.1102/1470-7330.2013.0015

36. Park HJ, Kim JH, Choi SY, et al. Prediction of Therapeutic Response of Hepatocellular Carcinoma to Transcatheter Arterial Chemoembolization Based on Pretherapeutic Dynamic CT and Textural Findings. *Am J Roentgenol*. 2017;209(4):W211–W220. doi:10.2214/AJR.16.17398

37. Tian Y, Hua H, Peng Q, et al. Preoperative Evaluation of Gd-EOB-DTPA-Enhanced MRI Radiomics-Based Nomogram in Small Solitary Hepatocellular Carcinoma (≤3 cm) With Microvascular Invasion: a Two-Center Study. *J Magn Reson Imaging*. 2022;56(5):1459–1472. doi:10.1002/jmri.28157

38. Zhao Y, Zhang J, Wang N, et al. Intratumoral and peritumoral radiomics based on contrast-enhanced MRI for preoperatively predicting treatment response of transarterial chemoembolization in hepatocellular carcinoma. *BMC Cancer*. 2023;23(1):1026. doi:10.1186/s12885-023-11491-0

39. Douhara A, Namisaki T, Moriya K, et al. Predisposing factors for hepatocellular carcinoma recurrence following initial remission after transcatheter arterial chemoembolization. *Oncol Lett*. 2017;14(3):3028–3034. doi:10.3892/ol.2017.6489

40. Wang B, Li F, Cheng L, et al. The pretreatment platelet count is an independent predictor of tumor progression in patients undergoing transcatheter arterial chemoembolization with hepatitis B virus-related hepatocellular carcinoma. *Future Oncol*. 2019;15(8):827–839. doi:10.2217/fon-2018-0591

41. Kuang Y, Li R, Jia P, et al. MRI-Based Radiomics: nomograms predicting the short-term response after transcatheter arterial chemoembolization (TACE) in hepatocellular carcinoma patients with diameter less than 5 cm. *Abdom Radiol*. 2021;46(8):3772–3789. doi:10.1007/s00261-021-02992-2

42. Sun Y, Bai H, Xia W, et al. Predicting the Outcome of Transcatheter Arterial Embolization Therapy for Unresectable Hepatocellular Carcinoma Based on Radiomics of Preoperative Multiparameter MRI. *J Magn Reson Imaging*. 2020;52(4):1083–1090. doi:10.1002/jmri.27143

43. Low HM, Lee JM, Tan CH. Prognosis Prediction of Hepatocellular Carcinoma Based on Magnetic Resonance Imaging Features. *Korean J Radiol*. 2023;24(7):660–667. doi:10.3348/kjr.2023.0168